MMSE Interference Suppression for Direct-Sequence Spread-Spectrum CDMA

Upamanyu Madhow and Michael L. Honig, *Senior Member, IEEE*

Abstract— **We consider interference suppression for direct-sequence spread-spectrum code-division multiple-access (CDMA) systems using the minimum mean squared error (MMSE) performance criterion. The conventional matched filter receiver suffers from the near-far problem, and requires strict power control (typically involving feedback from receiver to transmitter) for acceptable performance. Multiuser detection schemes previously proposed mitigate the near–far problem, but are complex and require explicit knowledge or estimates of the interference parameters. In this paper, we present and analyze several new MMSE interference suppression schemes, which have the advantage of being near–far resistant (to varying degrees, depending on their complexity), and can be implemented adaptively when interference parameters are unknown and/or time-varying. Numerical results are provided that show that these schemes offer significant performance gains relative to the matched filter receiver. We conclude that MMSE detectors can alleviate the need for stringent power control in CDMA systems, and may be a practical alternative to the matched filter receiver.**

I. INTRODUCTION

DEMODULATION of direct-sequence spread-spectrum (DS/SS) code-division multiple-access (CDMA) signals is conventionally achieved with a matched filter receiver. Because the crosscorrelations between the spreading, or signature, sequences for different transmissions are nonzero, a nearby interferer can disrupt reception of a highly attenuated desired signal. Interference suppression schemes previously proposed [5], [8]–[9], [14]–[16] can mitigate this *near–far problem* by exploiting the structure of the multiple-access interference. These schemes are significantly more complex than the matched filter receiver and require explicit knowledge or estimates of interference parameters. Consequently, recent proposals for CDMA systems (e.g., see [4]) assume a matched filter receiver, and solve the near–far problem by using power control, which requires feedback from the receiver to the transmitter.

In this paper we propose and analyze several interference suppression schemes based on the minimum mean squared error (MMSE) criterion. This work, originally presented in [10]–[11], was motivated by recent work which has shown that MMSE equalization techniques can be used to suppress both intersymbol interference (ISI) and crosstalk interference in wire channels [1], [7], [13]. A major advantage of MMSE schemes, relative to other previously proposed interference suppression schemes, is that explicit knowledge of interference parameters is not required, since filter parameters can be adapted to achieve the MMSE solution. Also, the complexity of these schemes, measured in number of filter coefficients, can be adjusted to achieve a given level of performance.

The MMSE linear detector for a pulse-amplitude modulated data signal in the presence of interfering data signals consists of a bank of filters matched to the pulse shapes of all active users followed by symbol-rate samplers and an Infinite-length Impulse Response (IIR) multi-input/single-output digital filter (see [7] and the references therein). The interference suppression schemes proposed here can be viewed as finite-complexity approximations of this detector. The first scheme proposed consists of sampling the channel output at the chip rate, and using an N-tap adaptive FIR filter to minimize the mean squared error (MSE) between the transmitted and detected symbol where N is the processing gain. This scheme is motivated by the fact that the MMSE linear detector just described can be implemented as an infinite-length fractionally spaced tapped-delay line. For the special case of symbol- and chip-synchronous CDMA transmissions, the N-tap detector is in fact equivalent to the MMSE linear detector. If, however, transmissions are symbol-asynchronous, then the MMSE linear detector requires an infinite number of taps. Furthermore, if transmissions are chip-asynchronous, then the MMSE linear detector requires that the tap spacing be smaller than the chip duration. However, our numerical results demonstrate that even in the chip- and symbol-asynchronous situation, the N-tap MMSE detector can offer a dramatic performance improvement relative to the matched filter detector. Finally, in the absence of multiple-access interference, the N-tap detector reduces to the conventional matched filter receiver.

The remaining interference suppression schemes proposed are motivated by the situation in which the processing gain N and the number of active users is large, but the number of strong interferers to be suppressed is relatively small. This may occur if power control alone cannot provide reliable protection against all strong interferers. The performance of the N-tap detector in ths situation may be degraded by slow convergence due to the large number of adaptive taps. We therefore consider simpler schemes for interference suppression that have fewer adaptive taps. In the first, the channel output is connected

Paper approved by J. S. Lehnert, the Editor for Modulation and Signal Design of the IEEE Communications Society. Manuscript received October 13, 1992; revised April 15, 1993. This paper was presented in part at the First International Conference Universal Personal Communications, Dallas, TX, September 28–October 1, 1992, and at the IEEE GLOBECOM, Orlando, FL, December 6–9, 1992.

U. Madhow was with Bell Communications Research, Morristown, NJ 07960 USA. He is now with the Coordinated Science Laboratory, University of Illinois, Urbana, IL 61801 USA.

M. L. Honig is with the Department of EECS, Northwestern University, Evanston, IL 60208 USA.

IEEE Log Number 9406144.

to a bank of D filters, each of which is a cyclically shifted version of the matched filter. In the second scheme a single matched filter is used, but its output is sampled D times per symbol interval. In each case, the decision statistic is a linear combination of the D samples obtained in a symbol interval, where the weights are selected to minimize the MSE. Since D can be much smaller than the processing gain N, these schemes should be easier to adapt than the N-tap MMSE detector when N is large. The first scheme typically performs somewhat better than the second scheme. Furthermore, the first scheme can be implemented as a bank of D filters of length N/D, which are each sampled D times per symbol interval. This makes the complexity of the two schemes comparable.

Interference suppression techniques for CDMA systems using the MMSE criterion have also been considered in [2], [5], [16], and [17]. An adaptive correlator, which is similar to the N-tap detector is proposed in [17]. However, the emphasis in [17] is on supressing narrowband interference, rather than other wideband CDMA signals.The detector proposed in [16] uses an MMSE criterion to estimate a *finite block* of transmitted symbols. The front end of this detector consists of a bank of filters matched to the pulse shapes of all active users followed by symbol-rate samplers. Explicit knowledge or estimates of the interference parameters are therefore assumed. Also, the estimated symbols are obtained by processing all matched filter outputs which correspond to the entire block of transmitted symbols. In contrast, the detectors presented here process samples from within a single symbol interval to estimate the desired symbol, and require significantly less computation.

The MMSE decision feedback equalizer (DFE) in the context of CDMA is considered in [2]. Since only decisions from the desired user are fed back, the feedback filter suppresses intersymbol interference, but not multiple-access interference. Since we focus on the latter in the present paper, we restrict attention to linear MMSE detectors of varying complexity. A multiuser decision-feedback detector, in which decisions on transmitted symbols from all users are fed back, is considered in [5]. Although the feedback filter in this case does suppress multi-user interference, this structure is more complex than the detectors considered in this paper, and is more difficult to adapt in the presence of unknown interferers.

As the level of background noise tends to zero, or as the energies of the interferers increases to infinity, the MMSE linear detector converges to the *decorrelating detector* introduced in [8]–[9], which eliminates multiple access interference at the expense of noise enhancement. Because the schemes considered here are finite complexity approximations of the MMSE linear detector, their performance is, in general, not as good as the performance of the decorrelating detector (which has the same complexity as that of the MMSE linear detector) [11]. Nevertheless, the results in Sections III and V demonstrate that the schemes considered here are generally near-far resistant, in the sense defined in [9].

The next section presents the CDMA system model considered, and the performance of the MMSE detectors presented in this paper is analyzed in Section III. Section IV presents the two simpler interference suppression schemes. Numerical results are presented and discussed in Section V, and Section VI contains our conclusions.

II. System Model

The received signal is the sum of K simultaneous CDMA transmissions plus additive white Gaussian noise. The received signal due to the jth user is given by

$$r_j(t) = \sqrt{2P_j} \sum_{i=-\infty}^{\infty} b_{i,j} s_j(t - iT - \nu_j) \cos(\omega_c t + \theta_j), \quad 1 \le j \le K \qquad (1)$$

where T is the bit interval, $b_{i,j} \in \{1, -1\}$ is the ith bit of the jth user, P_j, ν_j, and θ_j are the power, delay, and carrier phase of the jth user, respectively, ω_c is the carrier frequency, and $s_j(t)$ is a spreading, or signature, waveform given by

$$s_j(t) = \sum_{k=0}^{N-1} a_j[k]\psi(t - kT_c) \qquad (2)$$

where $a_j[k] \in \{-1, 1\}$ is the kth element of the spreading sequence for user j, $\psi(t)$ is the chip waveform, N is the processing gain, and $T_c = T/N$ is the chip duration. We assume that $\psi(t)$ has unit energy and duration T_c.

The received signal is then

$$r(t) = \sum_{j=1}^{K} r_j(t) + n(t) \qquad (3)$$

where $n(t)$ is white Gaussian noise with power spectral density $N_0/2$. The problem considered is to demodulate the first transmission, which will be referred to as the *desired transmission*. It is assumed that the receiver is synchronized to this transmission, so that the kth sample at the output of the chip matched filter is

$$r[k] = \sqrt{2} \int_{kT_c+\nu_1}^{(k+1)T_c+\nu_1} r(t)\psi(t)\cos(\omega_c t + \theta_1)\, dt. \qquad (4)$$

For the detectors considered in this paper all bit decisions are based on the discrete-time signal $r[k]$. (The notation $x[k]$ will be used to denote samples of a continuous-time signal spaced at the chip interval.)

We assume that the power and delay of the desired signal are, respectively, $P_1 = 1$ and $\nu_1 = 0$. For convenience we also consider a carrier-synchronous system in which the carrier phase $\theta_j = 0$ for each j, although our analysis is easily modified to take nonzero θ_j into account. For $2 \le j \le K$, the relative delay $\nu_j = (\tau_j + \delta_j)T_c$ where τ_j is an integer between 0 and $N-1$, and $\delta_j = \nu_j/T_c - \tau_j$ lies in the interval [0, 1). An asynchronous system is assumed in which both τ_j and δ_j may be nonzero.

Each detection scheme presented here estimates a given transmitted symbol from received samples within a single symbol period. The estimate of $b_{0,1}$ therefore depends only on the received signal for $t \in [0, T]$, or equivalently, the vector of received samples $\boldsymbol{r}^T = (r[0], \cdots, r[N-1])$. During this symbol interval the jth interfering signature sequence is modulated by symbol $b_{0,j}$ for $\nu_j < t \le T$, and by symbol $b_{-1,j}$ for $0 < t \le \nu_j$. From (1)–(4) it can be shown that

$$\boldsymbol{r} = b_{0,1}\boldsymbol{a}_1 + \sum_{j=2}^{K} \sqrt{P_j}(b_{0,j}\boldsymbol{a}_{0,j} + b_{-1,j}\boldsymbol{a}_{-1,j}) + \boldsymbol{n} \quad (5a)$$

where the N-vector $\boldsymbol{a}_j = (a_j[0], a_j[1], \cdots, a_j[N-1])^T$, and

$$[\boldsymbol{a}_{0,j}]_k = \phi_{1,j} a_j[k-\tau_j]\,\chi_{k \ge \tau_j} + \phi_{2,j} a_j[k-\tau_j-1]\,\chi_{k \ge \tau_j+1}$$

$$[\boldsymbol{a}_{-1,j}]_k = \phi_{1,j} a_j[k+N-\tau_j]\,\chi_{k \le \tau_j - 1} + \phi_{2,j} a_j[k+N-\tau_j-1]\chi_{k \le \tau_j} \quad (5b)$$

for $0 \le k \le N-1$ and $2 \le j \le K$ where χ_A is the indicator function for the set A, $\phi_{1,j} = \int_0^{T_c} \psi(t)\psi(t+\delta_j T_c)\,dt$ and $\phi_{2,j} = \int_0^{T_c} \psi(t)\psi[t+(1-\delta_j)T_c]\,dt$. The numerical results in Section V assume that $\psi(t)$ is a rectangular pulse of width T_c in which case $\phi_{1,j} = 1-\delta_j$ and $\phi_{2,j} = \delta_j$. The N-dimensional noise vector $\boldsymbol{n}$ is Gaussian with mean zero and covariance matrix $\sigma^2 \boldsymbol{I}_N$ where $\boldsymbol{I}_N$ denotes the $N \times N$ identity matrix, and $\sigma^2 = N_0/2$.

Note that $\boldsymbol{a}_{0,j}$ and $\boldsymbol{a}_{-1,j}$ are linearly independent and are modulated by different bits, so that the jth asynchronous interferer effectively contributes two interference vectors during a single symbol interval. We can therefore analyze the asynchronous system considered as a synchronous system with additional interferers.

III. Performance of Linear MMSE Detectors

Consider the problem of detecting the symbol b_1 given the received vector

$$\boldsymbol{r} = \sum_{j=1}^{L} b_j \boldsymbol{p}_j + \boldsymbol{n} \quad (6)$$

where $\boldsymbol{r} \in \mathbb{R}^M$, the vector $\boldsymbol{p}_1$ is the desired signal vector, b_j, $2 \le j \le L$, are symbols contributed by interferers, and $\{\boldsymbol{p}_j\}$, $j = 2, \cdots, L$, is the set of interference vectors. We will assume that $b_j \in \{-1, 1\}$, that the transmitted symbols are independent and have zero mean, and that the noise vector $\boldsymbol{n}$ is Gaussian with zero mean and covariance matrix Γ.

Comparing (5) and (6), it is clear that (6) applies to the asynchronous CDMA system considered in the last section where the dimension M is the processing gain N, $\Gamma = \sigma^2 \boldsymbol{I}_N$, the desired bit $b_1 = b_{0,1}$, the desired vector $\boldsymbol{p}_1 = \boldsymbol{a}_1$, and the set of interference vectors is $\{\sqrt{P_j}\boldsymbol{a}_{0,j},\ \sqrt{P_j}\boldsymbol{a}_{-1,j}\}$, $j = 2, \cdots, K$. The number of interference vectors $L-1$ can range from $K-1$ to $2(K-1)$, depending on the relative delays of the interfering transmissions.

The detection schemes proposed in this paper all have the form

$$\hat{b}_1 = \operatorname{sgn}(\boldsymbol{c}^T \boldsymbol{r}),$$

where $\boldsymbol{c} \in \mathbb{R}^M$ is chosen to minimize the mean squared error

$$\text{MSE} = E\{(\boldsymbol{c}^T\boldsymbol{r} - b_1)^2\} = (\boldsymbol{c}^T\boldsymbol{p}_1 - 1)^2 + \sum_{j=2}^{L} (\boldsymbol{c}^T\boldsymbol{p}_j)^2 + \boldsymbol{c}^T\Gamma\boldsymbol{c} \quad (7)$$

where the second equality follows from the assumption that the bits b_j are uncorrelated. For the N-tap MMSE detector, $\boldsymbol{r}$ in (6) and (5) are the same. Note that the matched filter detector corresponds to setting $\boldsymbol{c} = \boldsymbol{a}_1$. For the other detection schemes described in Section IV, the vectors $\boldsymbol{p}_j$ in (6) are different from the analogous vectors in (5), and the dimension M is less than the processing gain N.

In addition to MSE, two other performance measures of interest are signal-to-interference ratio (SIR) and error probability. The SIR is defined to be the ratio of the desired signal power to the sum of the powers due to noise and multiple-access interference at the output of the filter $\boldsymbol{c}$. That is,

$$\text{SIR} = \frac{(\boldsymbol{c}^T\boldsymbol{p}_1)^2}{\boldsymbol{c}^T\Gamma\boldsymbol{c} + \sum_{j=2}^{L}(\boldsymbol{c}^T\boldsymbol{p}_j)^2}. \quad (8)$$

It can be shown that the MMSE solution also maximizes the SIR. This maximum value is denoted by MSIR.

Since all users transmit binary, equiprobable, antipodal symbols, we may condition on $b_1 = 1$ for the purpose of evaluating the error probability $P(\hat{b}_1 \ne b_1)$. Conditioning further on the vector of interference bits $\boldsymbol{b}_I = (b_2, \cdots, b_L)^T$, we obtain

$$P_e(\boldsymbol{b}_I) = P(\hat{b}_1 \ne b_1 \mid b_1 = 1, \boldsymbol{b}_I) = Q\left(\frac{\boldsymbol{c}^T\boldsymbol{p}_1 + \sum_{j=2}^{K} b_j(\boldsymbol{c}^T\boldsymbol{p}_j)}{(\boldsymbol{c}^T\Gamma\boldsymbol{c})^{1/2}}\right) \quad (9)$$

where $Q(x) = (2\pi)^{-1/2}\int_x^\infty e^{-t^2/2}\,dt$. The *average* error probability is then given by $\overline{P}_e = E_{\boldsymbol{b}_I}\{P_e(\boldsymbol{b}_I)\}$. The *worst case* error probability is denoted as $P_e^* = P_e(\boldsymbol{b}_I^*)$ where $\boldsymbol{b}_I^*$ is the worst case interference bit pattern (for $b_1 = 1$), specified by $b_j^* = -\operatorname{sgn}(\boldsymbol{c}^T\boldsymbol{p}_j)$ for $2 \le j \le L$. A related performance measure that is considered later in this section is *near–far resistance* [8]–[9].

It is easily shown that the MMSE solution for $\boldsymbol{c}$ satisfies

$$\boldsymbol{A}\boldsymbol{c} = (1 - \boldsymbol{c}^T\boldsymbol{p}_1)\boldsymbol{p}_1. \quad (10)$$

where $\boldsymbol{A} = \sum_{j=2}^{L}\boldsymbol{p}_j\boldsymbol{p}_j^T + \Gamma$. All solutions to (10) minimize the MSE, whether or not $\boldsymbol{A}$ is nonsingular. Note that $\boldsymbol{A}$ is positive definite (and hence nonsingular) if either the noise covariance matrix Γ is positive definite or if the interference vectors $\{\boldsymbol{p}_j\}$, $j = 2, \cdots, K$, span $\mathbb{R}^M$. For nonsingular $\boldsymbol{A}$ it is shown in Appendix A that

$$\boldsymbol{c} = (1 + \boldsymbol{p}_1^T\boldsymbol{A}^{-1}\boldsymbol{p}_1)^{-1}\boldsymbol{A}^{-1}\boldsymbol{p}_1, \quad (11)$$

$$\text{MMSE} = 1 - \boldsymbol{c}^T\boldsymbol{p}_1 = (1 + \boldsymbol{p}_1^T\boldsymbol{A}^{-1}\boldsymbol{p}_1)^{-1}, \quad (12)$$

$$\text{MSIR} = \boldsymbol{c}^T\boldsymbol{p}_1/(1 - \boldsymbol{c}^T\boldsymbol{p}_1) = \boldsymbol{p}_1^T\boldsymbol{A}^{-1}\boldsymbol{p}_1 = \text{MMSE}^{-1} - 1. \quad (13)$$

If $L-1$, the number of interference vectors, is less than M, the dimension of the signal vectors, and the noise is zero (small), then the matrix $\boldsymbol{A}$ is singular (ill-conditioned). This situation is likely to apply to the N-tap detector, since $M = N$ is generally selected to be larger than $L-1 \le 2(K-1)$. In this case the following geometric derivation of the MMSE solution can be used to evaluate performance.

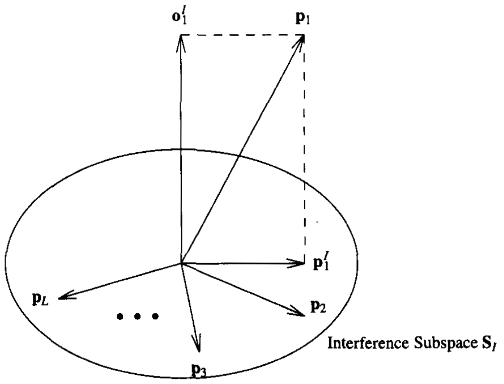

Fig. 1. Geometric representation of signal and interference vectors.

If $\boldsymbol{A}$ is ill-conditioned, then there are different solutions for $\boldsymbol{c}$ which result in nearly the same MSE. This can result in tap wandering during adaptation, which has been observed in single-user applications by Gitlin et al. [6]. One solution to this problem, which slightly increases the MSE, is the tap leakage algorithm proposed in [6].

A. Alternative Derivation Using Orthogonal Decompositions

In what follows it will be convenient to assume that the noise is white, i.e., that $\Gamma = \sigma^2 \boldsymbol{I}_M$. This assumption does not entail any loss of generality since the noise $\boldsymbol{n}$ can always be whitened by an orthonormal linear transformation $\boldsymbol{V}$ where $\boldsymbol{V}\Gamma\boldsymbol{V}^T = \sigma^2\boldsymbol{I}_M$, assuming Γ is positive definite.

Define the *interference subspace* $\boldsymbol{S_I}$ as the subspace of $\mathbb{R}^M$ spanned by the interference vectors $\boldsymbol{p}_2, \cdots, \boldsymbol{p}_L$, and let $\boldsymbol{S_I^O}$ denote the subspace of $\mathbb{R}^M$ orthogonal to $\boldsymbol{S_I}$. The desired vector $\boldsymbol{p}_1$ can then be expressed as

$$\boldsymbol{p}_1 = \boldsymbol{p}_1^I + \boldsymbol{o}_1^I, \tag{14}$$

where $\boldsymbol{p}_1^I$ denotes the projection of $\boldsymbol{p}_1$ onto $\boldsymbol{S_I}$ and $\boldsymbol{o}_1^I$ denotes the projection of $\boldsymbol{p}_1$ onto $\boldsymbol{S_I^O}$. Fig. 1 illustrates these geometric relationships. The MMSE solution $\boldsymbol{c}$ must lie in the subspace $\boldsymbol{S}$ spanned by the signal vectors $\boldsymbol{p}_1, \boldsymbol{p}_2, \cdots, \boldsymbol{p}_L$ since from (6), any vector $\boldsymbol{v}$ orthogonal to this space satisfies $\boldsymbol{v}^T\boldsymbol{r} = \boldsymbol{v}^T\boldsymbol{n}$, and therefore only contributes noise to the output. Furthermore, the space $\boldsymbol{S}$ is the direct sum of the orthogonal subspaces $\boldsymbol{S_I}$ and the subspace spanned by $\boldsymbol{o}_1^I$, so that the MMSE solution can be written as

$$\boldsymbol{c} = \boldsymbol{c}^I + d_1\boldsymbol{o}_1^I \tag{15}$$

where $\boldsymbol{c}^I$ is the projection of $\boldsymbol{c}$ onto $\boldsymbol{S_I}$, and d_1 is a scalar.

Projecting each side of (10) onto $\boldsymbol{S_I}$ and $\boldsymbol{S_I^O}$, and using (14) and (15) gives

$$\left(\sum_{j=2}^{L}\boldsymbol{p}_j\boldsymbol{p}_j^T + \sigma^2\boldsymbol{I}\right)\boldsymbol{c}^I = (1-\boldsymbol{c}^T\boldsymbol{p}_1)\boldsymbol{p}_1^I, \tag{16}$$

$$\sigma^2 d_1 = 1 - \boldsymbol{c}^T\boldsymbol{p}_1, \tag{17}$$

where we have used the fact that $\boldsymbol{c}^T\boldsymbol{p}_j = (\boldsymbol{c}^I)^T\boldsymbol{p}_j$ for $2 \le j \le L$. Solving (16)–(17) gives

$$d_1 = \frac{1-(\boldsymbol{c}^I)^T\boldsymbol{p}_1^I}{\sigma^2 + \|\boldsymbol{o}_1^I\|^2}, \quad \text{MMSE} = \frac{\sigma^2[1-(\boldsymbol{c}^I)^T\boldsymbol{p}_1^I]}{\sigma^2 + \|\boldsymbol{o}_1^I\|^2},$$
$$\text{MSIR} = \frac{\|\boldsymbol{o}_1^I\|^2 + \sigma^2(\boldsymbol{c}^I)^T\boldsymbol{p}_1^I}{\sigma^2[1-(\boldsymbol{c}^I)^T\boldsymbol{p}_1^I]}, \tag{18}$$

where $\boldsymbol{c}^I$ is given by

$$\left(\sum_{j=2}^{L}\boldsymbol{p}_j\boldsymbol{p}_j^T + \sigma^2 I\right)\boldsymbol{c}^I = \frac{\sigma^2[1-(\boldsymbol{c}^I)^T\boldsymbol{p}_1^I]}{\sigma^2 + \|\boldsymbol{o}_1^I\|^2}\boldsymbol{p}_1^I. \tag{19}$$

B. Asymptotic Behavior of the MMSE Solution

The quantities in (18)–(19) will be specified in terms of the crosscorrelations of the signal vectors $\boldsymbol{p}_1, \cdots, \boldsymbol{p}_L$; however, before doing this we consider the limiting behavior of the MMSE solution as 1) the noise level goes to zero, and 2) the interference vectors increase in energy. First consider the zero-noise situation in which $\sigma^2 = 0$. If $\boldsymbol{o}_1^I \neq 0$, then clearly the interference can be eliminated by choosing $\boldsymbol{c}$ to be a multiple of $\boldsymbol{o}_1^I$. This choice of $\boldsymbol{c}$ is called the *zero-forcing* solution. If $\sigma^2 = 0$, then the zero-forcing solution gives zero MSE, as indicated by (18). In this case, the MMSE solution is therefore

$$\boldsymbol{c} = \frac{\boldsymbol{o}_1^I}{\|\boldsymbol{o}_1^I\|^2} \tag{20}$$

where the scaling is determined by the requirement $|\boldsymbol{c}^T\boldsymbol{r}| = |\boldsymbol{c}^T\boldsymbol{p}_1| = |b_1| = 1$.

Now consider the *near–far* situation, in which the energy of one or more of the interference vectors can vary arbitrarily. Define $w_j = \|\boldsymbol{p}_j\|^2$ as the energy of the jth signal vector where $1 \le j \le L$. For a given w_1, we are interested in the MMSE solution $\boldsymbol{c}$ when the interference energies $w_2, \cdots, w_L$ assume values that *maximize* the MMSE. It is easily verified that the MMSE increases monotonically as a function of the interference energies so that we consider the asymptotic MMSE solution as $w_j \to \infty$ for $j \in J_\infty$, for some subset $J_\infty \subseteq \{2, \cdots, L\}$. In addition, we assume that w_j, $j \notin J_\infty$, are constant. In contrast to the worst case MMSE performance considered here, we note that for the maximum-likelihood detector, the interference energies that maximize error probability are not easily determined [14].

It is shown in Appendix B that the MMSE solution satisfies

$$\lim_{w_j \to \infty} \boldsymbol{c}^T\boldsymbol{p}_j = 0, \quad j \in J_\infty. \tag{21}$$

That is, $\boldsymbol{c}$ is asymptotically orthogonal to the space spanned by the set of interference vectors $\{\boldsymbol{p}_j\}$, $j \in J_\infty$. In the worst-case situation in which these vectors span the entire interference subspace $\boldsymbol{S_I}$, we have that $\boldsymbol{c}^I = 0$ asymptotically, and we obtain

$$\boldsymbol{c} = \frac{\boldsymbol{o}_1^I}{\|\boldsymbol{o}_1^I\|^2 + \sigma^2}, \quad \text{MMSE} = \frac{\sigma^2}{\|\boldsymbol{o}_1^I\|^2 + \sigma^2},$$
$$\text{MSIR} = \frac{\|\boldsymbol{o}_1^I\|^2}{\sigma^2}. \tag{22}$$

The MMSE solution is "near–far resistant" in the sense that the worst case MSIR in (22) is greater than zero provided that $\|\boldsymbol{o}_1^I\| > 0$. We now determine the near–far resistance of the MMSE solution in the sense defined in [8]–[9]. Let $\overline{P}_e(\sigma)$ be the average error probability for a given detector as a function of the noise variance σ^2. The *asymptotic efficiency* of the detector is defined in [8]–[9], [15] as

$$\gamma = \sup\left\{\kappa\colon \quad \lim_{\sigma\to 0} P_e(\sigma)/Q(\sqrt{\kappa w_1}/\sigma) \geq 0\right\}, \tag{23}$$

and is a limiting measure, as the noise level tends to zero, of how well the detector performs in the presence of multiple-access interference relative to its performance in the absence of multiple-access interference. The *near–far resistance* of the detector is defined in [8]–[9] as

$$\eta = \inf_{w_2,\cdots,w_L} \gamma. \tag{24}$$

That is, the near–far resistance is the asymptotic efficiency evaluated for *worst case* interference energies, and is a measure of the robustness of the detector with respect to variations in the received interference energies.

As $\sigma \to 0$, the error probability for the MMSE detector considered here satisfies

$$\lim_{\sigma\to 0} \frac{\overline{P}_e(\sigma)}{Q(\|\boldsymbol{o}_1^I\|/\sigma)} = \lim_{\sigma\to 0} \frac{P_e^*(\sigma)}{Q(\|\boldsymbol{o}_1^I\|/\sigma)} = 1. \tag{25}$$

The asymptotic efficiency of the MMSE detector is therefore $\|\boldsymbol{o}_1^I\|^2/w_1$. Since this quantity is independent of the energies of the interference vectors, we have that

$$\eta = \|\boldsymbol{o}_1^I\|^2/w_1. \tag{26}$$

The near–far resistance of the MMSE detectors considered is therefore the (appropriately normalized) norm of the component of the desired signal vector which is orthogonal to the space spanned by the interference vectors.

The near–far resistance is nonzero if and only if the desired vector $\boldsymbol{p}_1$ is not contained in the interference subspace $\boldsymbol{S_I}$. A necessary condition for this is to be true is that the dimension of $\boldsymbol{S_I}$ be strictly less than the dimension of the signal vectors M. Since the dimension of $\boldsymbol{S_I}$ is upper bounded by $L-1$, the number of interference vectors, it is reasonable to expect nonzero near–far resistance when $L-1 \leq M-1$. We emphasize that this is neither a necessary nor a sufficient condition for nonzero near–far resistance, but is merely an approximate rule. Applying this rule to the N-tap MMSE detector, the signal vector dimension $M = N$, so that this detector has enough degrees of freedom to suppress $(N-1)/2$ asynchronous interferers. (Recall that each asynchronous interferer can generate at most two interference vectors, so that $L-1 \leq 2(K-1)$). In contrast, for synchronous CDMA, the N-tap detector has enough degrees of freedom to suppress at most $N-1$ interferers, since each interferer generates only one interference vector $(L-1 = K-1)$.

C. MMSE Performance in Terms of Signal Energies and Cross-Correlations

Rewriting (18)–(19) in terms of signal energies and cross-correlations gives somewhat different (but equivalent) expressions for the MMSE solution $\boldsymbol{c}$, the MMSE, and MSIR than (11)–(13). Define the unit-energy signal vector $\overline{\boldsymbol{p}}_j$ by $\overline{\boldsymbol{p}}_j = w_j^{-1/2}\boldsymbol{p}_j$, and the normalized crosscorrelation between the jth and kth signals as $R_{jk} = \overline{\boldsymbol{p}}_j^T\overline{\boldsymbol{p}}_k$ where $1 \leq j,\, k < L$. Let $\boldsymbol{R}_I = (R_{jk})_{2\leq j,\, k\leq L}$ denote the nonnegative definite $(L-1)\times(L-1)$ interference cross-correlation matrix, and let $\rho^T = (R_{12}, \cdots, R_{1L})$ denote the vector of cross-correlations between the desired vector and the interference vectors.

We first compute $\boldsymbol{p}_1^I$ and $\boldsymbol{o}_1^I$. The projection of the desired signal onto the interference space $\boldsymbol{S_I}$ can be written as $\boldsymbol{p}_1^I = \sqrt{w_1}\sum_{j=2}^L z_j\overline{\boldsymbol{p}}_j$. To compute $\boldsymbol{z}^T = (z_2, \cdots, z_L)$ we note that

$$\overline{\boldsymbol{p}}_k^T\boldsymbol{o}_1^I = \overline{\boldsymbol{p}}_k^T(\boldsymbol{p}_1 - \boldsymbol{p}_1^I) = 0, \qquad 2 \leq k \leq L, \tag{27}$$

which gives

$$\boldsymbol{R}_I\boldsymbol{z} = \rho. \tag{28}$$

The vector $\boldsymbol{z}$ need not be unique unless the interference vectors are linearly independent, in which case $\boldsymbol{z} = \boldsymbol{R}_I^{-1}\rho$. It follows that

$$\boldsymbol{o}_1^I = \sqrt{w_1}\left(\overline{\boldsymbol{p}}_1 - \sum_{j=2}^L z_j\overline{\boldsymbol{p}}_j\right), \quad \text{and} \quad \|\boldsymbol{o}_1^I\|^2 = w_1(1-\rho^T\boldsymbol{z}). \tag{29}$$

From (26), the near–far resistance of the MMSE detector can be written as

$$\eta = 1 - \rho^T\boldsymbol{z} \tag{30}$$

where $\boldsymbol{z}$ is any vector that satisfies (28). It is easily shown that η is unique even if (28) does not have a unique solution.

To specify the MMSE solution we must compute $\boldsymbol{c}^I$. By definition,

$$\boldsymbol{c}^I = \sum_{j=2}^L d_j\overline{\boldsymbol{p}}_j, \tag{31}$$

where $\boldsymbol{d}_I^T = (d_2, \cdots, d_L)$ is determined from (19). It is shown in Appendix C that

$$\boldsymbol{d}_I = (\text{MMSE})\sqrt{w_1}\boldsymbol{e}_I \tag{32}$$

where $\boldsymbol{e}_I^T = (e_2, \cdots, e_L)$ satisfies

$$(\boldsymbol{R_I W_I R_I} + \sigma^2\boldsymbol{R}_I)\boldsymbol{e}_I = \rho, \tag{33}$$

and that

$$\text{MMSE} = [1 + w_1(1-\rho^T\boldsymbol{z})/\sigma^2 + w_1\rho^T\boldsymbol{e}_I]^{-1}, \tag{34}$$

$$\text{MSIR} = (w_1/\sigma^2)[(1-\rho^T\boldsymbol{z}) + \sigma^2\rho^T\boldsymbol{e}_I] \tag{35}$$

where the $(L-1)\times(L-1)$ matrix $\boldsymbol{W}_I = \text{diag}[w_2, \cdots, w_L]$. An important difference between (34)–(35) and the equivalent expressions (12)–(13) is that the vectors that appear in (34)–(35) have $L-1$ components, whereas the vectors in (12)–(13) have

$$P_e(\boldsymbol{b}_I) = Q\left(\frac{\sqrt{w_1/\sigma^2}(1-\rho^T\boldsymbol{z}+\sigma^2\rho^T\boldsymbol{e}_I)+\sigma^2\sum_{j=2}^{L}b_j\sqrt{w_j/w_1}[\boldsymbol{R}_I\boldsymbol{e}_I]_j}{(1-\rho^T\boldsymbol{z}+\sigma^4\boldsymbol{e}_I^T\boldsymbol{R}_I\boldsymbol{e}_I)^{1/2}}\right). \tag{36}$$

M components. The results for MSIR shown in Section V are computed from (35) when $L < M$ (for the N-tap detector), and from (13) when $L > M$ (for the simpler detection schemes to be described).

The error probability conditioned on the interfering symbols (and on $b_1 = 1$) can now be evaluated in a straightforward manner from (9), and is given by (36) at the top of the next page. The average and worst case error probabilities, with respect to the interfering symbols, can be computed from the preceding expression as described at the beginning of this section. Although the preceding performance measures are uniquely specified, the vectors $\boldsymbol{d}_I$ and $\boldsymbol{e}$ are unique if and only if the interference vectors are linearly independent.

IV. Simpler Interference Suppression Schemes

In practice, the N-tap MMSE detector would be implemented as an N-tap adaptive filter. In situations where the processing gain N is large, and the received energy per chip is low, rapid estimation of the MMSE vector $\boldsymbol{c}$ may be difficult. This motivates the following interference suppression schemes, which contain fewer adaptive taps.

A. Cyclically Shifted Filter Bank

Recall that the MMSE solution $\boldsymbol{c}$ for detecting b_1 in (6) can be written as $\boldsymbol{c} = \sum_{j=1}^{L}\alpha_j\boldsymbol{p}_j$ where $\alpha^T = (\alpha_1, \cdots, \alpha_L)$ is an appropriately chosen L-vector. If the interfering signals $\boldsymbol{p}_2, \cdots, \boldsymbol{p}_L$ were known, then the MMSE detector sign $(\boldsymbol{c}^T\boldsymbol{r})$ could be implemented by taking the inner product of the received vector with each of the signal vectors (or matched filters) $\boldsymbol{p}_j$, $j = 1, \cdots, L$, and then taking a linear combination of these outputs (i.e., weighted by the components of $\boldsymbol{\alpha}$).

The first reduced complexity interference suppression scheme consists of replacing the matched filters $\boldsymbol{p}_1, \boldsymbol{p}_2, \cdots, \boldsymbol{p}_L$ in the MMSE detector with a set of $D < N$ linearly independent vectors $\boldsymbol{p}_1, \boldsymbol{f}_1, \cdots, \boldsymbol{f}_{D-1}$, which are fixed *a priori*, and do not depend on the particular interference vectors (which are assumed to be unknown). The vector $\boldsymbol{c}$ defined in the last section is therefore restricted to have the form

$$\boldsymbol{c} = \alpha_0\boldsymbol{p}_1 + \sum_{j=1}^{D-1}\alpha_j\boldsymbol{f}_j \tag{37}$$

where the tap weights $\alpha_0, \cdots, \alpha_{D-1}$ are chosen to minimize $E[b_1 - \boldsymbol{c}^T\boldsymbol{r}]^2$. That is, $\boldsymbol{c} \in \mathbb{R}^N$ is now parametrized by the D-vector $(\alpha_0, \cdots, \alpha_{D-1})$. Notice that the choice $\alpha_0 = 1, \alpha_j = 0$, $1 \le j \le D-1$, is the standard matched filter.

The bank of D filters projects the original N-dimensional signal vectors onto a D-dimensional subspace. The near–far resistance of this D-tap detector equals that of the N-tap detector if and only if $\boldsymbol{o}_1^I$, the orthogonal component of the signal vector in N-dimensional space, is contained in the D-dimensional subspace spanned by $\boldsymbol{p}_1, \boldsymbol{f}_1, \cdots, \boldsymbol{f}_{D-1}$. If this condition is satisfied, then the D-tap detector can be made equivalent to the N-tap zero-forcing solution by selecting the α_j's in (37) so that $\boldsymbol{c}$ is a multiple of $\boldsymbol{o}_1^I$. This condition is not likely to be satisfied in general, so that the near–far resistance of the simpler D-tap scheme is typically strictly less than that of the N-tap detector.

Applying the approximate rule stated at the end of Section III.B, the effective signal vector dimension for the D-tap detector is $M = D$, so that there are enough degrees of freedom to suppress $(D-1)/2$ asynchronous strong interferers. This assumes that the filter vector $\boldsymbol{p}_1, \boldsymbol{f}_1, \cdots, \boldsymbol{f}_{D-1}$ are linearly independent. In order to reduce the complexity of this D-tap scheme, it is advantageous to select the vectors $\boldsymbol{f}_1, \cdots, \boldsymbol{f}_{D-1}$ to be cyclically shifted versions of the desired vector $\boldsymbol{p}_1$. For a typical set of user signature sequences (e.g., PN sequences), the resulting filter vectors are independent (in fact, nearly orthogonal).

The *cyclically shifted filter bank* (CSFB) scheme is illustrated in Fig. 2. The filter outputs are sampled at the symbol rate and are combined by means of D taps. Referring to the description of the CDMA system in Section II, the filters $\boldsymbol{f}_i \in \mathbb{R}^N$, $i = 0, \cdots, D-1$, are cyclic shifts of the signature sequence $\boldsymbol{a}_1$, i.e.,

$$[\boldsymbol{f}_i]_k = a_1[(k + i\Delta) \bmod N], \quad 0 \le k \le N-1, 0 \le i \le D-1. \tag{38}$$

Successive shifts are therefore spaced by $\Delta = \lfloor N/D \rfloor$. Defining $y_i = \boldsymbol{f}_i^T\boldsymbol{r}$, $0 \le i \le D-1$, from (5) we have that

$$\boldsymbol{y} = b_{0,1}\boldsymbol{s}_1 + \sum_{j=2}^{K}[b_{0,j}\boldsymbol{s}_{0,j} + b_{-1,j}\boldsymbol{s}_{-1,j}] + \boldsymbol{w} \tag{39}$$

where $\boldsymbol{y}^T = [y_0, \cdots, y_{D-1}]$,

$$[\boldsymbol{s}_1]_i = \boldsymbol{f}_i^T\boldsymbol{a}_1, \quad 0 \le i \le D-1, \tag{40a}$$

$$[\boldsymbol{s}_{k,j}]_i = \sqrt{P_j}\boldsymbol{f}_i^T\boldsymbol{a}_{k,j}, \quad 0 \le i \le D-1, k = 0, -1, 2 \le j \le K, \tag{40b}$$

and the noise vector has components $[\boldsymbol{w}]_i = \boldsymbol{f}_i^T\boldsymbol{n}$, $0 \le i \le D-1$, and has covariance matrix $\boldsymbol{U}$ with components $[\boldsymbol{U}]_{i,k} = \sigma^2\boldsymbol{f}_i^T\boldsymbol{f}_k$, $0 \le i, k \le D-1$. The decision rule is then

$$\hat{b}_{0,1} = \operatorname{sgn}(\boldsymbol{\alpha}^T\boldsymbol{y}), \tag{41}$$

where $\boldsymbol{\alpha} \in \mathbb{R}^D$ is chosen to minimize the MSE $= E\{(\boldsymbol{\alpha}^T\boldsymbol{y} - b_{0,1})^2\}$.

Clearly, (6) can be made equivalent to (39) by choosing the signal dimension $M = D$, the desired signal vector $\boldsymbol{p}_1 = \boldsymbol{s}_1$, the set of interference vectors $\boldsymbol{p}_2, \cdots, \boldsymbol{p}_L$ as $\{\boldsymbol{s}_{-1,j}, \boldsymbol{s}_{0,j}\}$, $2 \le j \le K$, and the noise covariance matrix $\Gamma = \boldsymbol{U}$. The performance of the CSFB scheme can therefore be evaluated

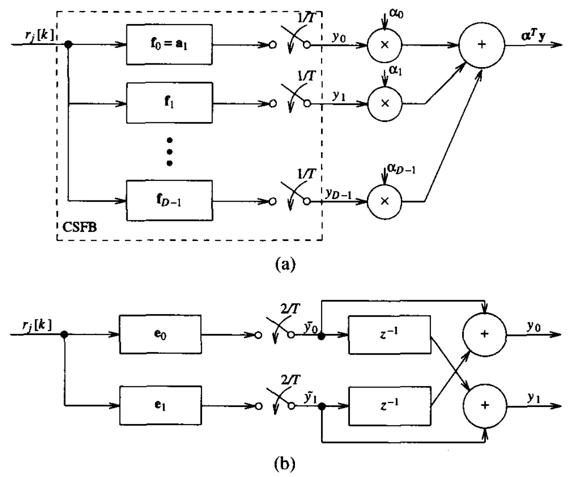

Fig. 2. (a) Detector with cyclically shifted filter bank. $\boldsymbol{f}_0, \cdots, \boldsymbol{f}_{D-1}$ are cyclic shifts of the matched filter $\boldsymbol{a}_1$. (b) Reduced complexity CSFB for $D = 2$.

from the formulas in Section III by making the appropriate substitutions.

We now show that the vector $\boldsymbol{y}$ can be generated with D filters each of length N/D, assuming that D divides N, so that the total number of taps in the filter bank is N, instead of ND. It is shown in Appendix D that the same reduction in complexity can be achieved even if D does not divide N (which is the case for the example used to generate our numerical results).

The output of the ith filter $\boldsymbol{f}_i$ after the zeroth symbol interval is

$$y_i = \sum_{j=0}^{N-1} a_1[(j + i\Delta) \bmod N] r[j] = \sum_{k=0}^{D-1} \sum_{j=0}^{\Delta-1} a_1[k + j\Delta] r[(k + (j - i)\Delta) \bmod N]. \quad (42)$$

We now divide each filter $\boldsymbol{f}_i$ into D disjoint contiguous *subfilters* of length N/D. The set of subfilters, which we denote as $\{\boldsymbol{e}_k\}$, $k = 1, \cdots, N/D$, is the same for each of the cyclically shifted filters f_i, and is specified by

$$[\boldsymbol{e}_j]_k = a_1[j + k\Delta], \quad 0 \le j \le \Delta - 1, 0 \le k \le D - 1. \quad (43)$$

Let $\tilde{y}_k[m]$ be the output of the kth subfilter $\boldsymbol{e}_k$ at time m. Then (42) and (43) imply that

$$y_i = \sum_{k=0}^{D-1} \tilde{y}_k[((k-i+1)\Delta-1) \bmod N], \quad 0 \le i \le D-1, \quad (44)$$

that is, y_i is the sum of the outputs of the subfilters $\boldsymbol{e}_k$, $k = 1, \cdots, D$, sampled at (chip) times $[(k-i+1)\Delta - 1] \bmod N$. To generate all D components of $\boldsymbol{y}$ the output of each $\{\boldsymbol{e}_k\}$ must be sampled D times at chip times iN/D, $i = 0, \cdots, D-1$. This is illustrated in Fig. 2(b) for the case $D = 2$. Of course, to detect the mth bit $b_{m,1}$ all chip samples used to generate the corresponding vector of filter outputs are incremented by mN.

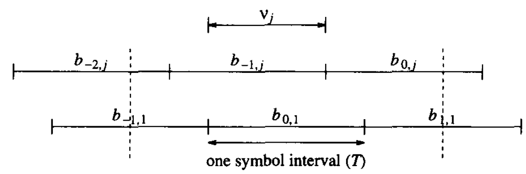

Fig. 3. Illustration of channel output samples $r[k]$, which are used to compute the estimated symbol $b_{0,1}$. The contribution to the channel output from the desired user and the jth interferer are shown. For the delay τ_j shown in the figure, the estimate $\hat{b}_{0,1}$ depends on the interference symbols $b_{-1,j}$, $b_{0,j}$, $b_{1,j}$, and $b_{-1,1}$.

B. Over-Sampling

The CSFB scheme is similar (but not equivalent) to sampling the output of the single matched filter $\boldsymbol{f}_0 = \boldsymbol{a}_1$ D times per symbol period. Over-sampling the output of the matched filter in this context is analogous to the fractionally spaced equalizer for single-user channels [7]. Denote the matched filter output at time $N - 1 - i\Delta$ as

$$\nu_i = \sum_{k=0}^{N-1} a_1[k] r[k - i\Delta] \quad (45)$$

where $\Delta = \lfloor N/D \rfloor$ is the interval between successive samples. The decision rule for $b_{0,1}$ is then given by $\hat{b}_{0,1} = \mathrm{sgn}(\boldsymbol{\alpha}^T \boldsymbol{v})$ where $\boldsymbol{v}^T = (\nu_{-m}, \cdots, \nu_0, \cdots, \nu_{D-m-1})$, m is a phase offset, and $\boldsymbol{\alpha} \in \mathbb{R}^D$ is chosen to minimize the MSE. In general, m can also be selected to minimize the MSE; however, the numerical results in the next section assume that $m = \lfloor (D-1)/2 \rfloor$. It is shown in Appendix E that the vector $\boldsymbol{v}$ can be expressed as shown in (6) where $\boldsymbol{p}_1, \cdots, \boldsymbol{p}_L$ are chosen appropriately. The performance of this scheme can therefore be evaluated by using the formulas in Section III.

From (45) it is apparent that samples $r[k]$ for $k = -(D - m - 1)\Delta, \cdots, N - 1 + m\Delta$ are used to compute the estimate $\hat{b}_{0,1}$. As illustrated in Fig. 3, depending on the relative delay τ_j, the jth interfering signal during this interval may contain segments from three different symbol intervals. The bits associated with these different segments are $b_{0,j}$, $b_{-1,j}$, and either $b_{-2,j}$ or $b_{1,j}$. This is in contrast to the CSFB and N-tap MMSE schemes, in which the jth interfering signal contributes segments from at most two successive symbol intervals with associated bits $b_{0,j}$ and $b_{-1,j}$. Also, for the over-sampling scheme adjacent symbol intervals of the desired transmission, associated with bits $b_{-1,1}$ and $b_{1,1}$, act as additional interference, which is not present in the CSFB scheme. For the same value of D the performance of the over-sampling scheme is therefore expected to be, on average, somewhat worse than that of the CSFB scheme. According to the approximate rule stated at the end of Section III-B, since each asynchronous interferer can effectively contribute three interference vectors, the over-sampling scheme should perform significantly better than the matched filter detector when the number of strong asynchronous interferers is less than or equal to $(D - 1)/3$.

Both the over-sampling and CSFB schemes require D filter taps. However, the CSFB scheme requires D samplers (as compared to one for the over-sampling scheme), together with D connections between sampled outputs as shown in Fig. 2(b). The increase in complexity required by the CSFB scheme relative to the over-sampling scheme seems quite modest so that the CSFB scheme may be preferable in many situations.

V. Numerical Results

We now compare numerically the performance of the interference suppression schemes discussed in preceding section with the matched filter receiver for a specific example. All of the following results assume that the processing gain $N = 31$, and that the interferers are asynchronous, but have the same signature sequence, which is different from the desired signature sequence. Both the desired and interference signature sequences are Gold sequences taken from [3, Table V]. The corresponding interference vectors are linearly independent, due to the different delays of the interferers, and the fact that distinct shifts of a PN sequence are linearly independent. The delays of the interferers relative to the desired signal, as multiples of the chip interval T_c, are denoted by $\nu_2, \cdots, \nu_K$. In order to reduce the computation required to average over all delays, we impose the relation $\nu_j = \nu_2 + (j-2)\lambda$ (modulo N) for $3 \leq j \leq K$, for fixed λ, which fixes the delay between user j, $j > 3$, and user 2. The following examples are averaged over ν_2.

Fig. 4 shows a plot of near–far resistance, as defined in Section III versus the delay ν_2 for the N-tap, CSFB, and over-sampling schemes. (The near–far resistance of the matched filter is zero.) The parameters are $K = 3$ users, $\lambda = 5.5$, and $D = 7$ for the CSFB and over-sampling schemes. According to the discussion in Section IV, the minimum number of taps for which the near–far resistance can be expected to be positive is $D = 5$ for the CSFB scheme and $D = 7$ for the over-sampling scheme. In fact, for $D = 5$ (not shown here), and for nearly all delays ν_2, the over-sampling scheme does have zero near–far resistance, and the near–far resistance of the CSFB scheme is quite small. Fig. 4 shows that the near–far resistance of each of the simpler schemes is very sensitive to delay, and can be quite small. In contrast, the near–far resistance of the N-tap MMSE detector is much less sensitive to delay, and stays relatively high. It is interesting that there are several delays at which the over-sampling scheme has greater near–far resistance than the CSFB scheme. However, the succeeding sets of numerical results, which are averaged over delays, show that the CSFB scheme offers a modest performance improvement relative to the over-sampling scheme.

We now consider the situation in which S (strong) interferers each have power P, assumed to be large, relative to the desired user, and the remaining $K - 1 - S$ interferers have the same power as the desired user. Figs. 5 and 6 show SIR and average error probability, respectively, as a function of P, which varies from 0 to 10 dB, relative to the desired user. The performance measures are averaged over the relative delay ν_2 (quantized to multiples of $T_c/4$). The signal-to-noise ratio for the desired user in the absence of multiple-access interference is fixed at 20 dB. The curves for the CSFB scheme, over-sampling scheme, and matched filter receiver assume that $K = 6$ and $S = 2$, whereas the curves for the N-tap MMSE detector assume that $K = 11$ and $S = 10$. That is, for the simpler schemes there are five interferers, two of which are strong, and for the N-tap MMSE detector there are 10 interferers, all of which are strong.

Ignoring the potential problem of slow adaptation speed, Figs. 5 and 6 show that the N-tap MMSE detector essentially eliminates the need for power control. Despite their relative simplicity, the CSFB and over-sampling schemes perform substantially better than the matched filter receiver, and would likely loosen the requirements for power control in this context. These results also show that for the same D the CSFB scheme performs somewhat better than the over-sampling scheme. We add that the degradation in the performance of the MMSE schemes with respect to single-user performance

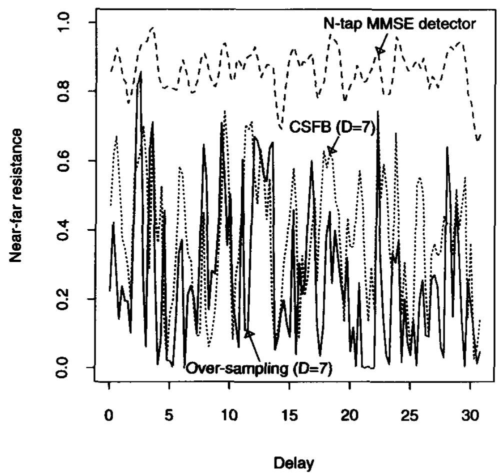

Fig. 4. Near–far resistance of MMSE detectors versus delay ν_2 ($N = 31$, $K = 3$).

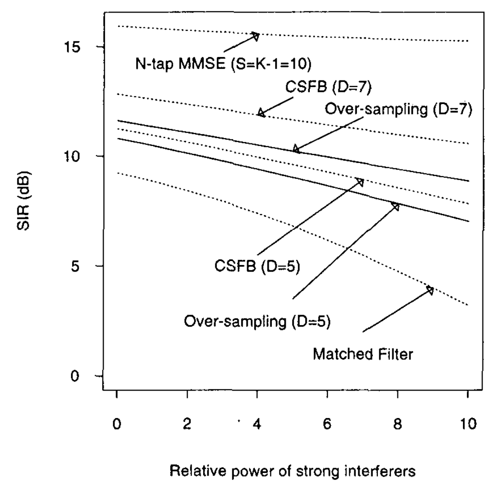

Fig. 5. SIR versus the relative power of strong interferers. For the N-tap MMSE detector ($N = 31$), $K = 11$ with 10 strong interferers, and for the simpler schemes, $K = 5$ with two strong interferers.

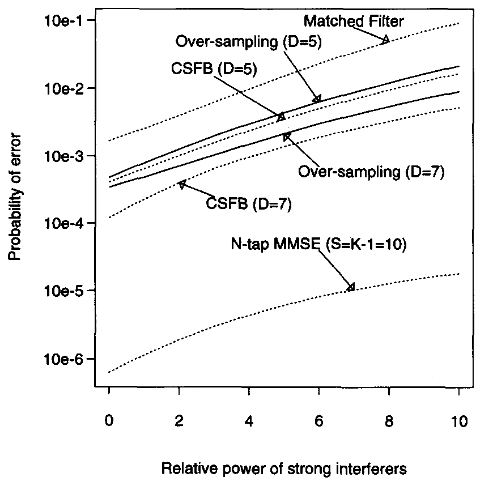

Fig. 6. Average error probability versus relative power of strong interferers. The parameters are the same as in Fig. 5.

was found to be nearly independent of SNR for values of SNR greater than 10 dB. Finally, all of the interference schemes considered can be combined with power control, and should result in a performance improvement relative to that of the matched filter receiver with the same degree of power control.

VI. Conclusion

We have presented three MMSE interference suppression schemes, which offer a significant performance improvement relative to the matched filter receiver. The N-tap MMSE detector seems appropriate when the processing gain N is relatively small, which corresponds to relatively few simultaneous transmissions. The CSFB and over-sampling schemes seem appropriate when N is relatively large, and there are relatively few strong interferers (because of power control). These detectors are significantly less complex than linear multiuser detectors previously proposed, such as the decorrelating detector [8]–[9], which in principle requires infinite memory. Of course, the MMSE schemes proposed here are easily modified so that the adaptive filter spans more than one symbol interval. This may be desirable if the adaptive filter is to suppress multi-path, as well as multiple-access, interference.

A major advantage MMSE interference suppression schemes have over previously proposed multiuser detection schemes [5], [8]–[9], [14] is that the MMSE performance criterion allows filter parameters to be adapted in a straightforward manner without *a priori* knowledge of the interference parameters. An important question is whether or not standard adaptive algorithms are able to track time-varying interference in a wireless environment. In addition to interference from other users, fading, multipath, and narrowband interference [12] must also be considered. Finally, the use of MMSE schemes to suppress both multiple-access interference and intersymbol interference in the context of CDMA with a finite bandwidth constraint is currently being studied.

Appendix

A. Derivation of (11)–(13)

Taking the inner product of each side of (10) with $\boldsymbol{c}$, we obtain

$$\boldsymbol{c}^T\boldsymbol{A}\boldsymbol{c} = \boldsymbol{c}^T\boldsymbol{p}_1(1-\boldsymbol{c}^T\boldsymbol{p}_1).$$

Substituting into the expression for MSE (7), and the expression for SIR (8) gives

$$\text{MMSE} = 1-\boldsymbol{c}^T\boldsymbol{p}_1,$$
$$\text{MSIR} = \boldsymbol{c}^T\boldsymbol{p}_1/(1-\boldsymbol{c}^T\boldsymbol{p}_1) = (1/\text{MMSE})-1. \tag{A.1}$$

Since the MSE is a quadratic function of $\boldsymbol{c}$, (10) is a necessary and sufficient condition for minimizing the MSE. If $\boldsymbol{A}$ is singular, then all solutions to (10) yield the same MSE and SIR. If $\boldsymbol{A}$ is nonsingular, so that $\boldsymbol{c}$ is unique, then the MMSE condition (10) can be rewritten as

$$\boldsymbol{c} = (1-\boldsymbol{c}^T\boldsymbol{p}_1)\boldsymbol{A}^{-1}\boldsymbol{p}_1. \tag{A.2}$$

Taking the inner product of each side with $\boldsymbol{p}_1$ gives

$$\boldsymbol{c}^T\boldsymbol{p}_1 = (1-\boldsymbol{c}^T\boldsymbol{p}_1)\boldsymbol{p}_1^T\boldsymbol{A}^{-1}\boldsymbol{p}_1.$$

Solving for $\boldsymbol{c}^T\boldsymbol{p}_1$, and substituting into (A.1)–(A.2) gives (11)–(13).

B. Proof of (21)

We first note that

$$\lim_{w_j\to\infty} \boldsymbol{c}^T\bar{\boldsymbol{p}}_j = 0, \quad j\in J_\infty. \tag{B.1}$$

That is, if $(\boldsymbol{c}^T\bar{\boldsymbol{p}}_j)^2 \geq \epsilon$ for some $j \in J_\infty$ and some $\epsilon > 0$, then $(\boldsymbol{c}^T\boldsymbol{p}_j)^2 \geq \epsilon w_j \to \infty$. Combining this with (7) contradicts the fact that MMSE ≤ 1 ($\boldsymbol{c} = 0$ gives MSE = 1).

Denote the space spanned by $\{\boldsymbol{p}_j\}$, $j \in J_\infty$, as $\boldsymbol{S}_\infty$, and denote the projection of $\boldsymbol{c}$ onto $\boldsymbol{S}_\infty$ as $\boldsymbol{c}^\infty$. (B.1) implies that as $w_j \to \infty$, $j \in J_\infty$, $\boldsymbol{c}^\infty \to 0$. Consequently,

$$\lim_{\substack{w_j\to\infty\\ j\in J_\infty}} (\boldsymbol{c}^\infty)^T\boldsymbol{p}_i = 0, \qquad i\notin J_\infty, \tag{B.2}$$

since $((\boldsymbol{c}_\infty^T\boldsymbol{p}_i)^2 \leq w_i\|\boldsymbol{c}^\infty\|^2$, and the w_i are bounded for $i \notin J_\infty$.

To establish (21) we project each side of (10) onto $\boldsymbol{S}_\infty$ to obtain

$$\sum_{j=2}^{L}(\boldsymbol{c}^T\boldsymbol{p}_j)\boldsymbol{p}_j^\infty + \sigma^2\boldsymbol{c}^\infty = (1-\boldsymbol{c}^T\boldsymbol{p}_1)\boldsymbol{p}_1^\infty, \tag{B.3}$$

$1 \leq j \leq L$ where the projection of $\boldsymbol{p}_j$ onto $\boldsymbol{S}_\infty$ is denoted as $\boldsymbol{p}_j^\infty$. Premultiplying each side of (B.3) by $(\boldsymbol{c}^\infty)^T$ gives

$$\sum_{j=2}^{L}(\boldsymbol{c}^T\boldsymbol{p}_j)[(\boldsymbol{c}^\infty)^T\boldsymbol{p}_j^\infty] + \sigma^2\|\boldsymbol{c}^\infty\|^2 = (1-\boldsymbol{c}^T\boldsymbol{p}_1)[(\boldsymbol{c}^\infty)^T\boldsymbol{p}_1^\infty]. \tag{B.4}$$

Combining this with (B.2) and using the fact that $\boldsymbol{c}^T\boldsymbol{p}_j = (\boldsymbol{c}^\infty)^T\boldsymbol{p}_j^\infty$ for $j \in J_\infty$ gives

$$\sum_{j\in J_\infty}[(\boldsymbol{c}^\infty)^T\boldsymbol{p}_j]^2 + \sigma^2\|\boldsymbol{c}^\infty\|^2 \to 0, \tag{B.5}$$

as $w_j \to \infty$, $j \in J_\infty$, which implies (21).

C. Derivation of (32)–(35)

It is convenient to rewrite (16) as

$$\left(\sum_{j=2}^{L} w_j \bar{\boldsymbol{p}}_j \bar{\boldsymbol{p}}_j^T + \sigma^2 \boldsymbol{I}\right) \boldsymbol{c}^I = \xi \boldsymbol{p}_1^I \tag{C.1}$$

where ξ denotes the MMSE from (12). Substituting from (31) gives

$$\sum_{j=2}^{L}\sum_{k=2}^{L} w_j R_{jk} d_k \bar{\boldsymbol{p}}_j + \sigma^2 \sum_{k=2}^{L} d_j \bar{\boldsymbol{p}}_j = \xi \boldsymbol{p}_1^I, \tag{C.2}$$

and taking the inner product of each side with $\bar{\boldsymbol{p}}_m$ for $2 \leq m \leq L$ gives (32)–(33). From (12) and (15) we have that

$$1 - \xi = \boldsymbol{c}^T \boldsymbol{p}_1 = (\boldsymbol{c}^I)^T \boldsymbol{p}_1 + d_1 (\boldsymbol{o}_1^I)^T \boldsymbol{p}_1. \tag{C.3}$$

Substituting (17) for d_1, and (31) and (32) for $(\boldsymbol{c}^I)^T$ gives

$$1 - \xi = \xi w_1 \rho^T \boldsymbol{e}_I + \frac{\xi \|\boldsymbol{o}_1^I\|^2}{\sigma^2}, \tag{C.4}$$

which implies (34) and (35).

D. Complexity Reduction for CSFB: General Case

We show that the vector $\boldsymbol{y}$ can be generated with $D-1$ filters of length Δ, and one of length $\Delta + \delta$ where $\delta = N - D\Delta$. The output of $\boldsymbol{f}_i$ at time $N-1$ is

$$\begin{aligned} y_i &= \sum_{k=0}^{N-1} a_1[(k + i\Delta) \bmod N] r[k] \\ &= \sum_{k=0}^{i-1}\sum_{m=0}^{\Delta-1} a_1[m + k\Delta] r[m + N + (k-i)\Delta] \\ &\quad + \sum_{k=i}^{D-2}\sum_{m=0}^{\Delta-1} a_1[m + k\Delta] r[m + (k-i)\Delta] \\ &\quad + \sum_{m=0}^{\Delta-1+\delta} a_1[m + (D-1)\Delta] \\ &\quad \cdot r[m + (D-1-i)\Delta + \delta], \end{aligned} \tag{D.1}$$

for $0 \leq i \leq D-1$. Define the subfilter $\boldsymbol{e}_{D-1}$ by

$$[\boldsymbol{e}_{D-1}]_m = a_1[m + (D-1)\Delta], \quad 0 \leq m \leq \Delta - 1 + \delta. \tag{D.2}$$

The subfilters $\boldsymbol{e}_0, \cdots, \boldsymbol{e}_{D-2}$ are again defined by (43). Let $\tilde{y}_k[m]$ denote the output of the filter $\boldsymbol{e}_k$ at time m. From (D.1) we have that

$$\begin{aligned} y_i &= \sum_{k=0}^{i-1} \tilde{y}_k[N - 1 - (i-k-1)\Delta] \\ &\quad + \sum_{k=i}^{D-2} \tilde{y}_k[(k-i+1)\Delta - 1] + \tilde{y}_{D-1}[N - 1 - i\Delta] \end{aligned} \tag{D.3}$$

which expresses y_i as the sum of the outputs of the filters $\boldsymbol{e}_1, \cdots, \boldsymbol{e}_{D-1}$ at appropriate chip times.

E. Over-Sampling Solution and Performance

The aperiodic crosscorrelation between the signature sequences $\boldsymbol{a}_k$ and $\boldsymbol{a}_i$ is denoted as

$$C_{j,k}(i) = \begin{cases} \sum_{m=0}^{N-1-i} a_j[m] a_k[m+i], & 0 \leq m \leq N-1, \\ \sum_{m=0}^{N-1+i} a_j[m-i] a_k[m], & -(N-1) \leq i < 0, \\ 0, \quad |i| > N. \end{cases} \tag{E.1}$$

From (45) and (5) $\boldsymbol{v}$ can be written as

$$\begin{aligned} \boldsymbol{v} &= b_{0,1}\boldsymbol{s}_{0,1} + b_{-1,1}\boldsymbol{s}_{-1,1} + b_1 \boldsymbol{s}_{1,1} + \sum_{j=2}^{K} \{b_{0,j}\boldsymbol{s}_{0,j} \\ &\quad + b_{-1,j}\boldsymbol{s}_{-1,j} + b_{1,j}\boldsymbol{s}_{1,j} + b_{-2,j}\boldsymbol{s}_{-2,j}\} + \boldsymbol{w}, \end{aligned} \tag{E.2}$$

for $1 \leq j \leq K$ where

$$\begin{aligned} [\boldsymbol{s}_{k,j}]_i = \sqrt{P_j}\{\phi_{1,j} C_{j,1}(i\Delta + \tau_j + kN) + \delta_{2,j} \\ \cdot C_{j,1}(i\Delta + \tau_j + 1 + kN)\}, \end{aligned} \tag{E.3}$$

the index i takes on values $-m, \cdots, 0, \cdots, D-m-1$, $\tau_1 = \delta_1 = 0$, and $P_1 = 1$. Comparing (E.2) with (6), the vector $\boldsymbol{s}_{1,0}$ is the desired vector, and the remaining vectors are interference vectors (including $\boldsymbol{s}_{-1,1}$ and $\boldsymbol{s}_{1,1}$ from user 1). Note that for each $2 \leq j \leq K$, either $\boldsymbol{s}_{1,j}$ or $\boldsymbol{s}_{-2,j}$ must be zero. The Gaussian noise vector $\boldsymbol{w}$ has zero mean and $D \times D$ covariance matrix $\boldsymbol{U}$ with components

$$[\boldsymbol{U}]_{i,k} = \sigma^2 C_{1,1}(|i-k|\Delta). \tag{E.4}$$

Note that the performance of the CSFB scheme can similarly be expressed in terms of crosscorrelations between interfering signature sequences and cyclic shifts of the desired signature sequence.

REFERENCES

[1] M. Abdulrahman and D. D. Falconer, "Cyclostationary crosstalk suppression by decision feedback, equalization on digital subscriber loops," *IEEE J. Select. Areas Commun.*, vol. 10, pp. 640–649, Apr. 1992.

[2] M. Abdulrahman, D. D. Falconer, and A. U. H. Shekh, "Equalization for interference cancellation in spread spectrum multiple access systems," in *Proc. VTC*, May 1992.

[3] F. D. Garber and M. B. Pursley, "Optimal phases of maximal sequences for asynchronous spread-spectrum multiplexing," *IEE Electron. Lett.*, vol. 16, no. 19, pp. 756–757, Sept. 1980.

[4] K. S. Gilhousen *et al.*, "On the capacity of a cellular CDMA system," *IEEE Trans. Veh. Technol.*, vol. 40, pp. 303–311, May 1991.

[5] A. Duel-Hallen, "Decorrelating decision-feedback multiuser detector for synchronous code-division multiple-access channel," *IEEE Trans. Commun.*, vol. 41, pp. 285–290, Feb. 1993.

[6] R. D. Gitlin, H. C. Meadows, and S. B. Weinstein, "The tap-leakage algorithm: An algorithm for the stable operation of a digitally implemented, fractionally spaced, adaptive equalizer," *Bell Syst. Tech. J.*, vol. 61, no. 8, pp. 1817–1839, Oct. 1982.

[7] M. L. Honig, P. Crespo, and K. Steiglitz, "Suppression of near- and far-end crosstalk by linear pre- and post-filtering," *IEEE J. Select. Areas Commun.*, vol. 10, pp. 614–629, Apr. 1992.

[8] R. Lupas and S. Verdú, "Linear multi-user detectors for synchronous code-division multiple-access channels," *IEEE Trans. Inform. Theory*, vol. 35, pp. 123–136, Jan. 1989.

[9] ——, "Near-far resistance of multi-user detectors in asynchronous channels," *IEEE Trans. Commun.*, vol. 38, pp. 496–508, Apr. 1990.

[10] U. Madhow and M. L. Honig, "Minimum mean squared error interference suppression for direct-sequence spread-spectrum code-division multiple-access," in *Proc. 1st Int. Conf. Universal Personal Commun.*, Dallas, TX, Sept. 28–Oct. 1, 1992.

[11] ——, "Error probability and near-far resistance of minimum mean squared error interference suppression schemes for CDMA," in *Proc. IEEE Global Telecommun. Conf.*, Orlando, FL, Dec. 6–9, 1992.

[12] L. B. Milstein, "Interference rejection techniques in spread spectrum communications," *Proc. IEEE*, vol. 76, pp. 657–671, June 1988.
[13] B. R. Petersen and D. D. Falconer, "Minimum mean square equalization in cyclostationary and stationary interference—Analysis and subscriber line calculations," *IEEE J. Select. Areas Commun.*, vol. 9, pp. 931–940, Aug. 1991.
[14] S. Verdú, "Minimum probability of error for asynchronous Gaussian multiple-access channels," *IEEE Trans. Inform. Theory*, vol. IT-32, pp. 85–96, Jan. 1986.
[15] ——, "Optimum multi-user asymptotic efficiency," *IEEE Trans. Commun.*, vol. 38, no. 4, pp. 496–508, Apr. 1990.
[16] Z. Xie, R. T. Short, and C. K. Rushforth, "A family of suboptimum detectors for coherent multi-user communications," *IEEE J. Select Areas Commun.*, vol. 8, pp. 683–690, May 1990.
[17] C. N. Pateros and G. J. Saulnier, "Adaptive correlator receiver performance in direct-sequence spread spectrum communications," in *Proc. MILCOM '92*, pp. 17.3.1-17.3.5.

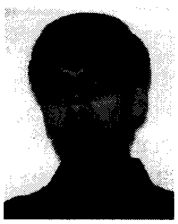

Upamanu Madhow received the B.S. degree in electrical engineering from the Indian Institute of Technology, Kanpur, in 1985. He received the M.S. and Ph.D. degrees in electrical engineering from the University of Illinois, Urbana-Champaign in 1987 and 1990, respectively.

From August 1990 to July 1991, he was a Visiting Assistant Professor at the University of Illinois. From August 1991 to July 1994, he was a research scientist at Bell Communications Research. Since August 1994, he has been with the University of Illinois at Urbana-Champaign, where he is currently an Assistant Professor. His current research interests are in communication systems and networks for wireless mobile communications, and in high speed computer communication networks.

Dr. Madhow was awarded the President of India Gold Medal for graduating at the top of his undergraduate class. He was the recipient of a University of Illinois fellowship from 1985 to 1986, and a Schlumberger fellowship from 1987 to 1988.

Michael L. Honig (S'80–M'81–SM'92) was born in Phoenix, AZ, in 1955. He received the B.S. degree in electrical engineering from Stanford University in 1977, and the M.S. and Ph.D. degrees in electrical engineering from the University of California, Berkeley, in 1978 and 1981, respectively.

He subsequently joined Bell Laboratories, Holmdel, NJ, where he worked on local area networks, adaptive filtering, and voiceband data transmission. In 1983 he joined the Systems Principles Research Division at Bellcore, where he worked on Digital Subscriber Lines and wireless communications. He has also been a visiting lecturer at Princeton University. Since Fall 1994, he has been with Northwestern University, where he is currently the Ameritech Professor in Information Technology in the Electrical Engineering and Computer Science Department.